MOSS LANDING MARINE LABORATORIES
CALIFORNIA STATE UNIVERSITY FRESNO. HAYWARD. SACRAMENTO. SAN FRANCISCO. SAN JOSE. STANISLAUS

P. O BOX 450
MOSS LANDING CA USA
95039-0450
(408) 633-3304

December 14, 1989

Dr. Edward J. Green
Office of Naval Research
Code 1122C
800 N. Quincy St.
Arlington, VA 22217-5000

RE: Annual Report on ONR Grant N00014-86-G-0147

Dear Ed,

During the past two years, we have worked on the development of simple, rapid methods for the analysis of trace metals in seawater while on board ship, and continued to develop our capabilities for analyses of dissolved chemicals in situ. Previous work performed with support from ONR resulted in the development of methods for the determination of cobalt and copper in seawater. These analyses were performed using the technique of flow injection analysis with chemiluminescence detection. In the period from October 1988 to the present, we have extended this work by developing analytical techniques for the determination of manganese and iron in seawater.

We have developed a method for the determination of manganese that is based on its catalysis of the oxidation of 7,7,8,8-tetracyanoquinodimethan. The chemiluminescence produced by this reaction allows us to detect manganese at concentrations down to 0.1 nM with no significant interferences in seawater. Each analysis requires only 6 minutes and is completely automated. The results obtained with this technique are indistinguishable from those obtained by preconcentration and graphite furnace atomic absorption spectrometry (Figure 1). We have used this method to study manganese geochemistry in the coastal zone and in deep-sea hydrothermal vent plumes. We are also completing the development of a method for the determination of iron in seawater.

The oxidation of brilliant sulfoflavine in the presence of iron(II) generates chemiluminescence, which can be used to determine iron concentrations to concentrations of at least 0.3 nM. Further work to reduce a persistent blank at this level should lower the detection limit. This technique allows the determination of iron redox speciation because the method is selective only for iron(II). Total iron concentrations can be obtained by adding ascorbic acid to samples, which results in the rapid reduction of iron(III). This method was used to determine iron redox speciation in hydrothermal vent plumes with great success on a cruise to the Juan de Fuca Ridge.

Partial contents: Continuous determination of nitrate concentrations in situ, and

tracer for vertical advection (EDC)

area in August, 1989 (Figure 2).

Analytical techniques that were developed in our laboratory for cobalt, copper, and hydrogen peroxide analyses were used in studies of the biogeochemical processes that regulate these chemicals in the ocean. The results of these investigations were published during this reporting period. This work included a study of trace metal cycles in a basin the Southern California Borderland (Johnson et al., 1988) and the photochemistry of hydrogen peroxide and nutrients in the Mediterranean Sea (Johnson et al., 1989; Lohrenz et al., 1988).

We have completed the development of an upgraded submersible chemical analyzer (Scanner) systems during this period. The system have been tested at sea and a manuscript describing the results has been submitted (Johnson et al., 1989). The instrument is capable of resolving small features (< 5 m) at lowering rates up to 40 m min^{-1} with high precision (relative standard deviation of >1%). Continued development of the system has resulted in an instrument that is substantially easier to operate and more reliable than earlier versions. The upgraded Scanner was also used to make continuous measurements of manganese and iron distributions in hydrothermal vent plumes (Figure 3).

Finally, we have developed a simple method for the generation of numerical models of biogeochemical cycling in the ocean. This involves the use of electronic spreadsheet programs such as Lotus 1-2-3 to program the differential equations for the time-dependent differential equation for advection-diffusion-reaction models. A numerical model for the distribution of manganese along the VERTEX east-west transect was developed. This model allows the manganese concentrations to be predicted to within 25% over a 3000 km long section (Figure 4). The inputs to the model are the rates of manganese input or removal due to eolian deposition, phytoplankton uptake, organic carbon regeneration, scavenging onto sinking particles and rates of mixing and advection.

We intend to keep working along similar lines over the next year. This will include participation in the Martin/Duce cruise across the equator, where we will use these methods to make continuous measurements of iron, cobalt and manganese in the water column and in solar incubation experiments.

Sincerely yours,

Kenneth S. Johnson

Kenneth S. Johnson
Professor of Chemical Oceanography

Enclosures: Reference List
Figures
Reprints

Kenneth S. Johnson, 1/88-12/89

Figures

Figure 1. The concentration of dissolved manganese determined on board ship 100 km off the California coast (36° 25'N; 123° 07'W) by FIA-CL. The profile of dissolved manganese determined 5 years previously at the nearby VERTEX station 1 (35.8°N; 122.6°W) is shown for comparison (Martin et al., 1985).

Figure 2. Dissolved iron (II) concentrations plotted versus total (II + III) dissolved iron concentrations in the same samples from hydrothermal plumes on the Juan de Fuca Ridge. Note that at high concentrations (A) the increase in iron is essentially all in the +II oxidation state (except for two anomalous samples), while at low concentrations (B) most of the iron is in the +III state.

Figure 3. Contoured sections of dissolved manganese (A) and temperature anomaly (B) measured on a vertical tow of a rosette equipped with a CTD-transmissometer-Scanner package through a vent plume on the Juan de Fuca Ridge. The contour interval for Mn is 20 nM to a maximum of 220 nM and the interval for temperature is 0.01°C to a maximum of 0.08°C. The time axis is in units of 5 seconds. The total elapsed time was 5.5 hours and the package was towed a distance of 12 km across the ridge crest during this time. The dotted line shows the tow path of the rosette package.

Figure 4. The distribution of dissolved manganese measured (A) along the east-west VERTEX transect (Martin et al., 1985) and the concentrations calculated with a numerical for two limiting cases. In (B) the manganese maximum at 700 m is produced by a flux from margin sediments. In (C) the manganese maximum is produced by a decrease in the scavenging rate in the oxygen minimum and there is no flux from the sediments.
Figure 11. Dissolved iron concentrations versus the concentration of suspended particulate matter in the samples at stations over the continental shelf from Monterey Bay to Pt. Arena (Martin and Gordon, 1988).

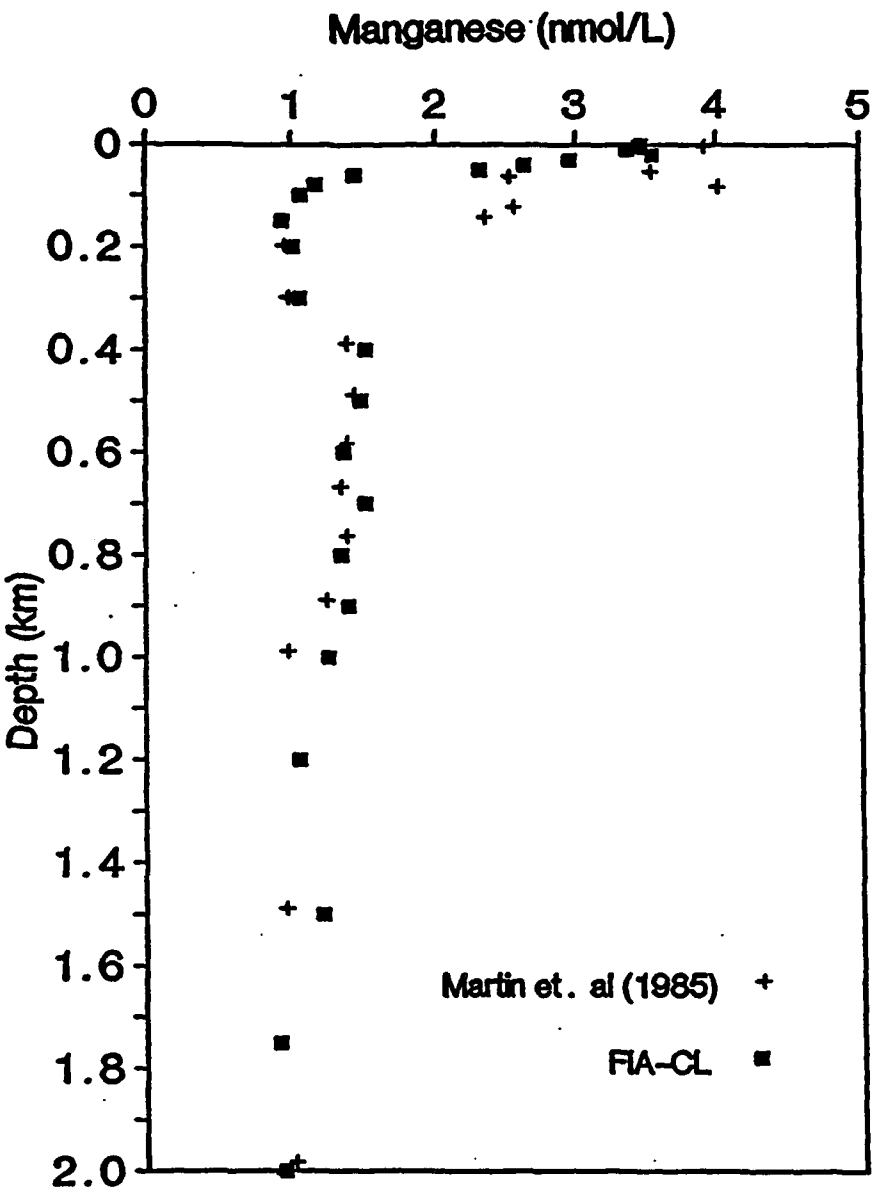
Manganese (nmol/L)
0
1
2
3
4
5
0
0.2
0.4
0.6
0.8
1.0
1.2
1.4
1.6
1.8
2.0
Depth (km)
Martin et. al (1985)
FIA-CL

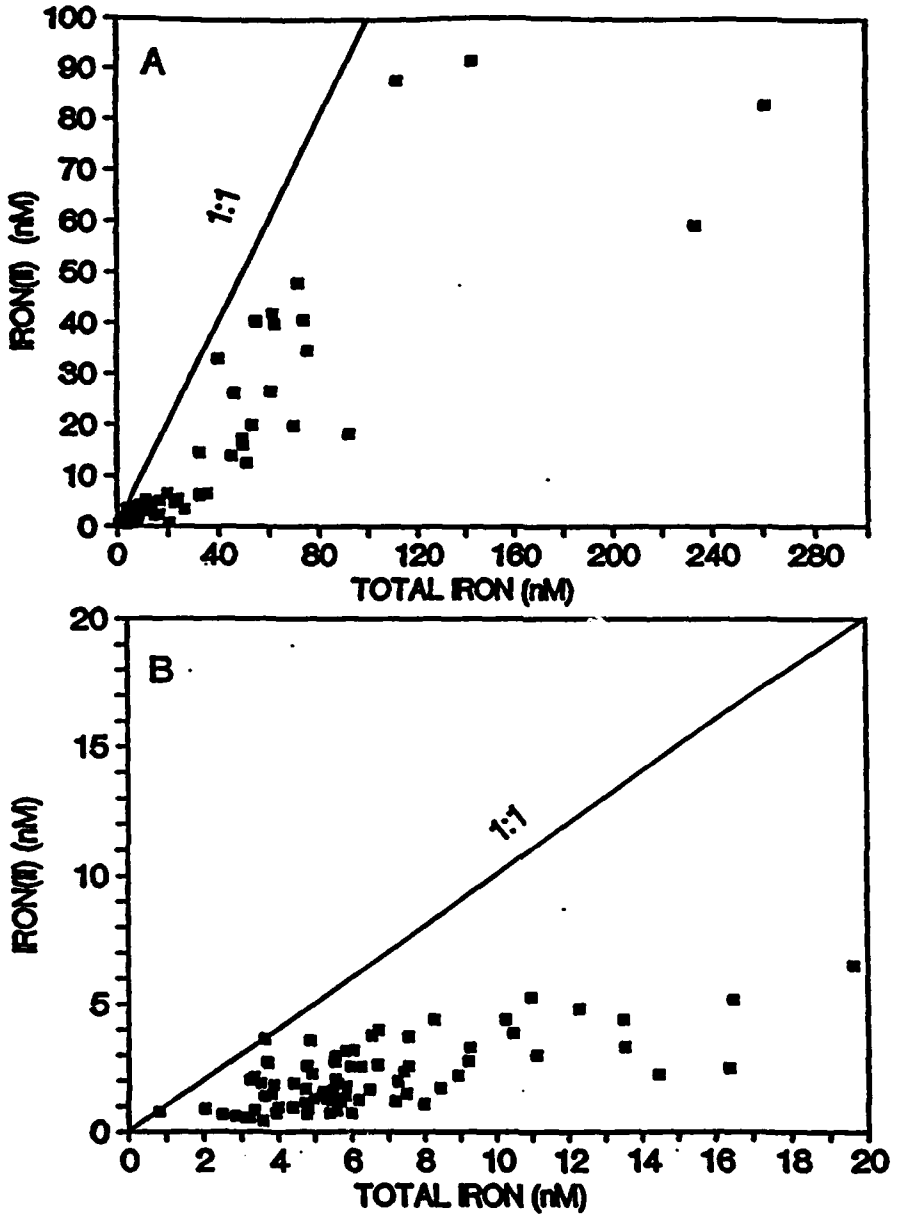
A
1:1
IRON(II) (nM)
TOTAL IRON (nM)
0
10
20
30
40
50
60
70
80
90
100
0
40
80
120
160
200
240
280
B
1:1
IRON(II) (nM)
TOTAL IRON (nM)
0
5
10
15
20
0
2
4
6
8
10
12
14
16
18
20

Manganese (nmol/L)

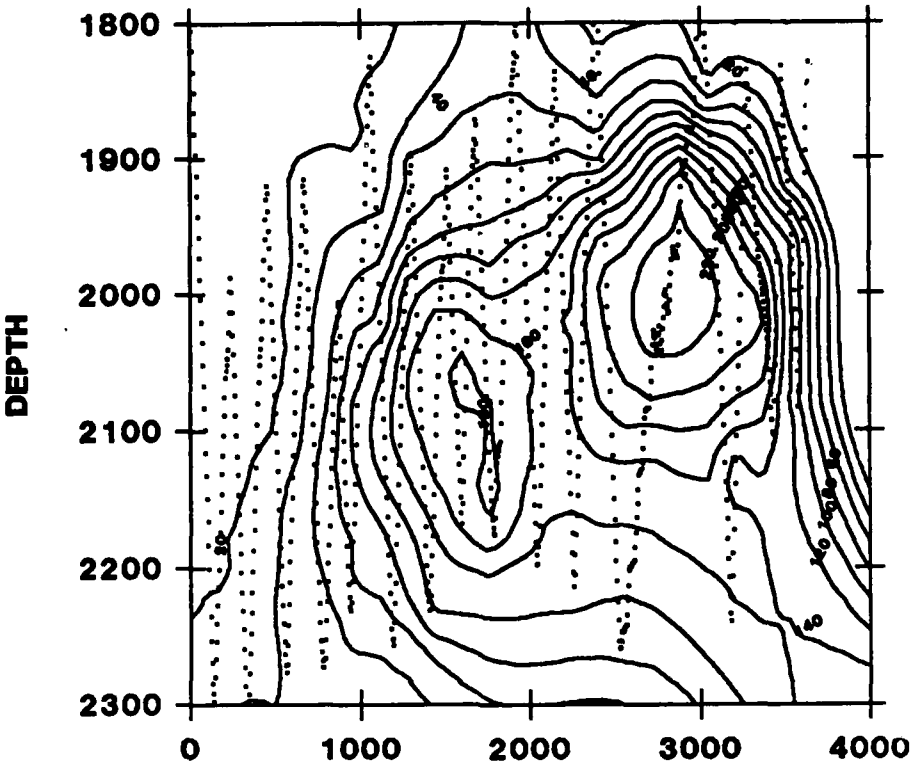

Temperature Anomaly (°C)

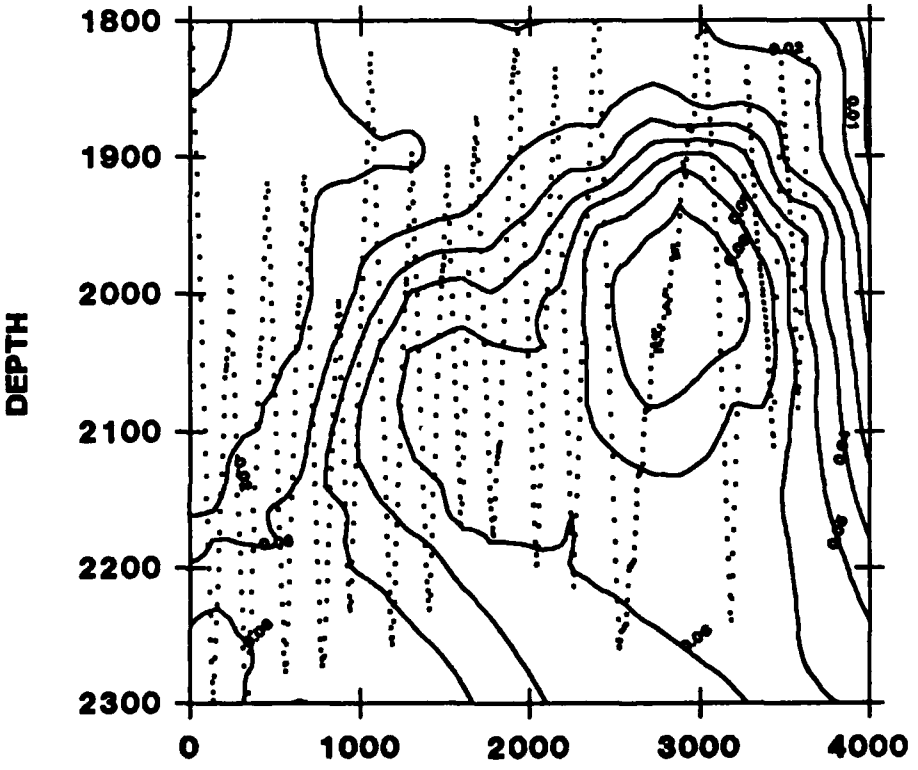

TIME

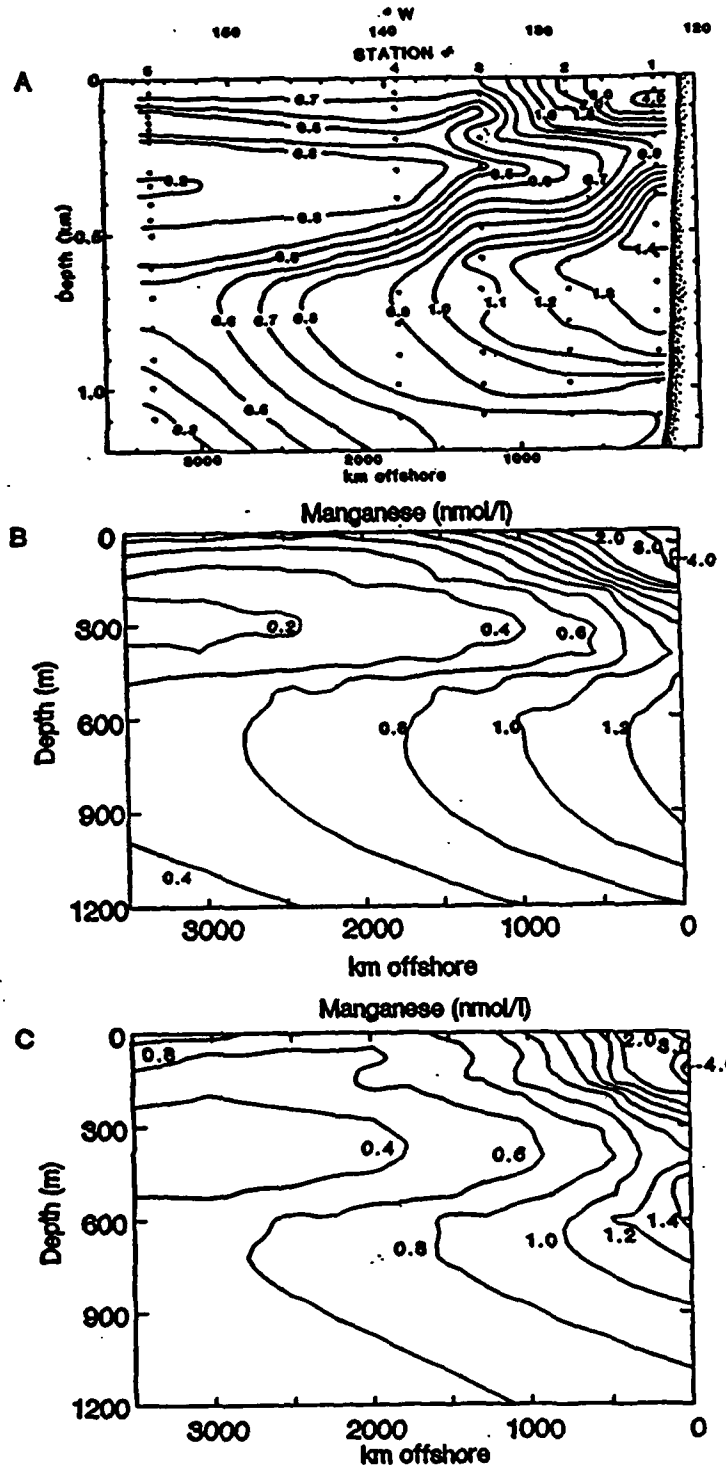

A. Observed Mn Section, Martin et al., 1985.

B. High Transport Model.

C. Low Transport Model.

Kenneth S. Johnson, 1/88-12/89

Papers Published

Johnson, K. S., P. S. Stout, W. M. Berelson and C. M. Sakamoto-Arnold. 1988. Cobalt and copper distributions in the waters of Santa Monica Basin, California. Nature, 332, 527-530.

Lohrenz, S. E., D. A. Wiesenburg, I. P. DePalma, K. S. Johnson and D. E. Gustafson, Jr. 1988. Interrelationships among primary production, chlorophyll, and environmental conditions in frontal regions of the Western Mediterranean Sea. Deep-Sea Research, 35, 793-810.

Johnson, K. S. 1988. The influence of the sediment community on chemical transformations. Applied Geochemistry, 3, 115.

Johnson, K. S., S. W. Willason, D. A. Wiesenburg, S. E. Lohrenz and R. A. Arnone. 1989. Hydrogen peroxide in the Western Mediterranean Sea: a tracer for vertical advection. Deep-Sea Research, 36, 241-254.

Johnson, K. S., C. M. Sakamoto-Arnold and C. L. Beehler. 1989. Continuous determination of nitrate concentrations in situ. Deep-Sea Research, 36, 1407-1413.

Invited Conference Presentations

Johnson, K. S. 1988. Automated and in situ chemical analyses of seawater. Invited presentation at U. S. Global Ocean Flux Study, Pacific Planning Meeting, February 2-3, 1988.

Johnson, K. S. 1988. In situ chemical sensors for detecting and exploring hydrothermal vents. Invited paper presented at, Workshop on In-situ Chemical Sensors for Detecting and Exploring Ocean Flocr Hydrothermal Vents, Woods Hole Oceanographic Institution, Woods Hole, Massachusetts, June 28-30, 1988.

Johnson, K. S. 1989. A submersible chemical analyzer (Scanner): continuous chemical measurements in deep-sea hydrothermal vents and the oceanic water column. Invited presentation at OCEANS '89, September 18-21, Seattle, Washington.

Contributed Conference Presentations

Johnson, K. S., P. M. Stout, C. M. Sakamoto-Arnold and W. M. Berelson. 1988. Cobalt and copper distributions in the waters of Santa Monica Basin. Trans. Am. Geophys. Union, 68, 1682. Presented at American Geophysical Union/American Society of

Kenneth S. Johnson, 1/88-12/89

Limnology and Oceanography Ocean Sciences Meeting, New Orleans, Louisiana, Jan. 18-22, 1988.

Stout, P. M. and K. S. Johnson. 1988. Cobalt distributions in coastal and pelagic regions of the Pacific Ocean. Trans. Am. Geophys. Union, 68, 1754. Presented at American Geophysical Union/American Society of Limnology and Oceanography Ocean Sciences Meeting, New Orleans, Louisiana, Jan. 18-22, 1988.

Stout, P. M., K. S. Johnson, K. C. Coale and C. M. Sakamoto-Arnold. 1988. Shipboard determination of copper in seawater using flow injection analysis with chemiluminescence detection. Transactions of the American Geophysical Union, 69, 1264. Oral presentation at American Geophysical Union Fall Meeting, San Francisco, Dec. 6-11, 1988.

Johnson, K. S. 1989. Trace Metal Determination by Flow Injection Analysis with Chemiluminescence Detection. Poster presentation at Gordon Research Conference on Chemical Oceanography, August 14-18, 1989, Meriden, New Hampshire.

Johnson, K. S. 1989. Continuous Measurements of Chemical Concentrations In Situ. Poster presented at The Oceanography Society, August 27-30, Monterey, California.

Deep-Sea Research, Vol. 36, No. 9, pp. 1407–1413, 1989.
Printed in Great Britain.

0198-0149/89 $3.00 + 0.00

Continuous determination of nitrate concentrations *in situ*

KENNETH S. JOHNSON,*† CAROLE M. SAKAMOTO-ARNOLD† and CARL L. BEEHLER‡

(*Received* 11 *January* 1989; *in revised form* 26 *April* 1989; *accepted* 16 *May* 1989)

Abstract—A submersible chemical analyser (Scanner) was used to measure nitrate concentrations *in situ* to depths of nearly 2000 m. Nitrate anomalies with a vertical span of 5 m can be detected at lowering rates up to 40 m min^{-1}. The nitrate concentrations measured *in situ* are in good agreement with hydrographic data collected by conventional means at the same location. The relative standard deviation of the analyses performed *in situ* is ±0.79%. The method can be easily extended to most other colorimetric analyses.

INTRODUCTION

THE widespread availability of continuous profiling instruments for physical and biological properties (conductivity, temperature, pressure, pigment fluorescence and light transmission) has radically changed our understanding of oceanographic processes. However, instruments capable of continuously measuring the concentrations of dissolved chemicals have not been widely available. Only electrochemical sensors for *in situ* measurements of dissolved oxygen and pH have been developed (FOYN, 1965; BEN-YAAKOV and KAPLAN, 1968). Measurements made with these electrochemical sensors have shown small-scale structure (e.g. BEN-YAAKOV and KAPLAN, 1968; KESTER *et al.*, 1973) that would be missed by conventional hydrographic sampling techniques. These variations in pH and oxygen reflect the variety of physical, chemical and biological processes that occur in the ocean. Instruments that measure dissolved nutrient and trace chemical concentrations *in situ* with high resolution could be applied to the study of a broad range of oceanographic processes. Such uses might include studies of chemical fluxes through the water column and from sediments, chemical transformations, factors regulating primary production and ocean circulation.

Our laboratory has recently developed a submersible chemical analyser (Scanner) that is capable of measuring dissolved chemical concentrations *in situ* by colorimetric analysis (JOHNSON *et al.*, 1986a, 1988). The Scanner uses an unsegmented continuous flow analysis manifold to collect the sample, add the reagents and deliver the analyte species to the detector.

The purpose of the work described here was to test the utility of the Scanner for measuring dissolved chemical concentrations in the upper ocean. We report results for vertical profiles of the concentrations of the micronutrient compound nitrate. We have

* Moss Landing Marine Laboratories, P.O. Box 450, Moss Landing, CA 95039, U.S.A.
† Monterey Bay Aquarium Research Institute, 160 Central Avenue, Pacific Grove, CA 93950, U.S.A.
‡ Marine Science Institute, University of California, Santa Barbara, CA 93106, U.S.A.

focused our work on nitrate because of the important function this chemical has in controlling oceanic primary production on short time scales.

METHODS

Apparatus

Sea tests were conducted in the Southern California Bight aboard the R.V. *Pt. Sur*. The Scanner design and components have been previously described by JOHNSON *et al.* (1986b). Several modifications were made to increase the reliability of the Scanner. The two most important changes are a new motor for the peristaltic pump and the addition of a third standard selection valve. The extra valve allows three standard solutions to be analysed *in situ* so that non-linearity in standard curves can be assessed. The pump motor was replaced with a digital stepper motor (Digital Motors, Inc., HY-200-3450) driven by a microstep controller (Centent Co., CN0142). The stepper motor and the standard selection valves were pressure compensated using a fluorocarbon liquid (Dupont, Fluorinert FC-43). This system does not suffer from the arcing problems that plague conventional DC brush motors that are operated in a liquid environment. The Scanner was powered by a battery consisting of 12 Gates (0820-0004) lead-acid cells. This battery provided enough power for more than 24 h of continuous operation at a typical current of 0.5 A and 24 V. A Seabird SB-4 CTD was attached to the Scanner frame to determine salinity, temperature and depth.

The concentration of nitrate was determined by the conventional technique of reducing nitrate to nitrite with a cadmium column and measuring the nitrite as an azo dye. No attempt was made to correct for nitrite concentrations and the values reported therefore correspond to nitrate + nitrite. The reagents were prepared as described by JOHNSON and PETTY (1983), except that imidazole (0.1 M imidazole and 12 mM $CuSO_4$) was used as the buffering agent and the cadmium was hand filed from sticks of the pure metal. The coarse, hand-filed cadmium allowed a longer column (3 cm) to be used. The reduction efficiency was constant for week-long periods of time. The reaction manifold for the nitrate analysis is shown in Fig. 1. The lag time for water to flow from the inlet to the detector was 65 s. A low dead-volume, polypropylene filter (Alltech no. 32171) was placed on the sample inlet to prevent clogging by gelatinous material in the water column.

Nitrate concentrations were also measured in samples collected from 5 liter Niskin bottles suspended on a rosette. These discrete samples were frozen and returned to the

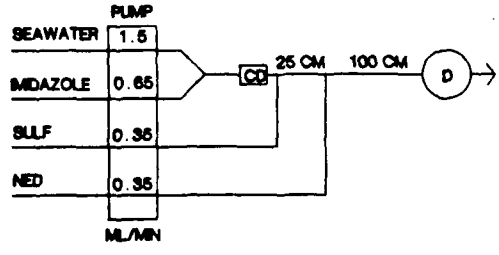

Fig. 1. Flow manifold for the determination of nitrate. Numbers refer to the length (cm) of the 0.8 mm i.d. teflon tubing used to construct the manifold. CD is the cadmium column and D is the colorimetric detector.

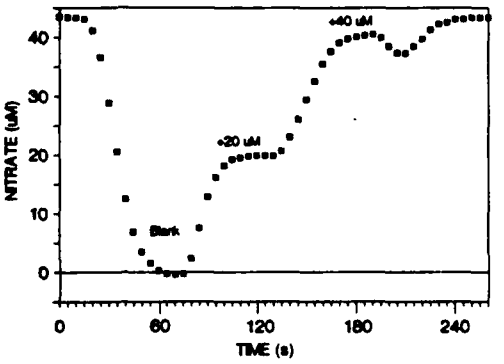

Fig. 2. Analyses of nitrate standards (low nutrient seawater blank, blank +20 μM NO_3 and blank +40 μM NO_3) performed near a depth of 1800 m. The dip after the analysis of the high standard is an artifact caused by the presence of a small amount of blank solution that remains in the sample line. This small volume of blank is rapidly flushed from the system and after that time undiluted sample passes through the detector.

laboratory where they were analysed by flow injection analysis (JOHNSON and PETTY, 1983).

Instrument calibration

Three standard solutions prepared in low nutrient surface seawater (+0, +20 and +40 μM) were analysed *in situ* every 24 min to calibrate the Scanner. Each solution was drawn into the analytical manifold for a 1 min period, which resulted in a 15–20 s long plateau in the detector output (Fig. 2). These calibrations were used to assess the effects of temperature and pressure on the extent of reaction in the flow system (JOHNSON *et al.*, 1986b) and to compensate for instrumental drift. Temperature and pressure can influence the results by changing rates of reaction (JOHNSON *et al.*, 1986b). Most analytical reactions do not go to completion in a flow injection system and a change in reaction rates will alter the amount of color that is formed. The absorbances of the nitrate standards were independent of the temperature and pressure changes. Apparently, this reaction is complete in the time it takes for the sample and reagent mixture to reach the detectors. This is not true for other chemical analyses that we have performed using the Scanner (JOHNSON *et al.*, 1986b).

Detector voltages were digitized and stored every 5 s. The data were processed through three steps before the final concentrations were obtained. First, raw detector voltages, which are proportional to light transmittance, were converted to absorbance values and time shifted to correct for the lag in the response of each channel. Second, a calibration curve was fitted to each set of standard absorbances and concentrations. A linear fit was found to be adequate. Finally, sample concentrations were calculated from the absorbance values using a linear interpolation between the two most recent calibration curves. The final concentrations reported here were not smoothed.

RESULTS AND DISCUSSION

Vertical profiles of nitrate were determined in Santa Cruz Basin in the Southern California Bight. This basin is isothermal from its sill depth of 1050 m to the bottom near

1900 m. Oxygen concentrations are sufficiently high in the basin that little or no nitrate reduction can occur in the water column. As a result, the subsill waters have a uniform nitrate concentration. Measurements below the sill depth should, therefore, give a good indication of the precision of the analyses.

The Scanner was lowered and raised at a rate of 20 m min^{-1} in the upper 200 m of the water column and at 40 m min^{-1} below that. The nitrate profiles that were obtained (Figs 3 and 4) show the trends expected for typical nutrient distributions in the ocean: lowest values occurred near the surface, nitrate increased rapidly through the thermocline and concentrations increased slowly with depth below the thermocline. Nitrate concentrations at the surface ranged from 1 to 5 μM during the time we occupied the station. Upwelling was presumably occurring in the vicinity as surface nitrate concentrations were as high as 13 μM at some locations. As expected, the concentrations measured below the sill depth are constant (43.0 ± 0.3 μM, 1 S.D., n = 566), and nearly identical values were found on both the down- and up-casts (down, 43.1 ± 0.3 μM; up, 42.9 ± 0.4 μM).

The nitrate concentrations determined *in situ* showed the same trend as the values determined on samples collected from a conventional hydrographic cast (Fig. 3). The two sets of data were offset throughout the profile, however. The difference (39.7 ± 0.9 μM, n = 10 vs 43.0 ± 0.3 μM, n = 566) is significant in the subsill waters. A calibration error must be present in one or both sets of data. Previous analyses of nitrate in the subsill waters of Santa Cruz Basin have ranged from 39 to 41 μM (BERELSON, 1985). It is not clear, therefore, in which set of data the error lies.

The upper 100 m of the profiles are shown in Fig. 4. The spike near the surface in the nitrate data on the down-cast was presumably an artifact due to the passage of a small air

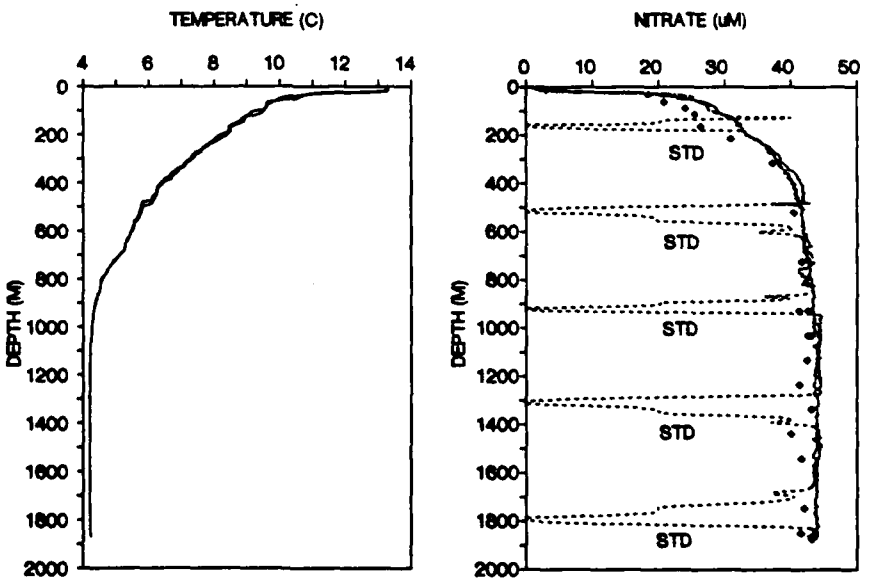

Fig. 3. Vertical profiles of nitrate and temperature measured in the Santa Cruz Basin (33°39.1N, 119°32.8W, 6 June 1988). Analyses of standard solutions are marked STD and shown by a dashed line. Nitrate concentrations measured in samples collected from Niskin bottles at the same location are shown as diamonds. Both the up- and down-casts are shown.

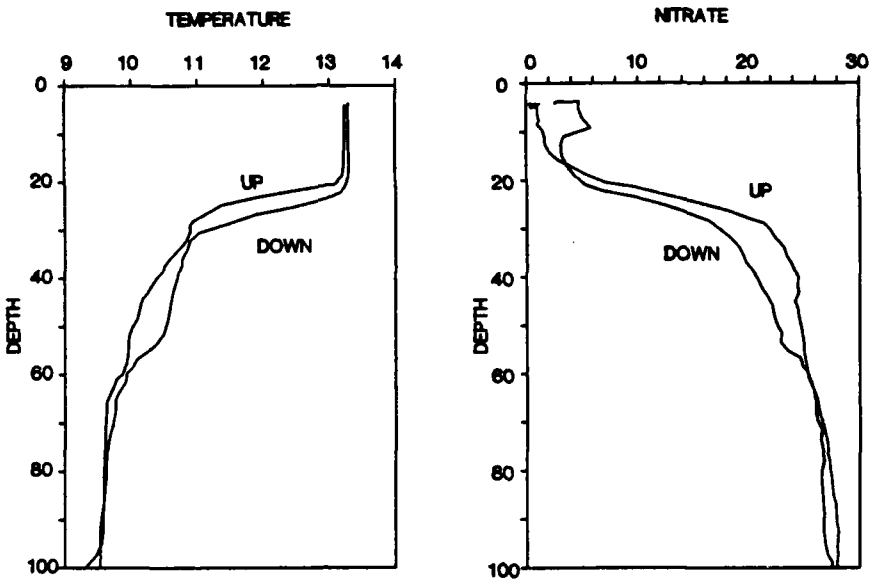

Fig. 4. Surface nitrate and temperature data from Fig. 3 plotted vs depth.

bubble through the flow cell. Similar spikes were found in many of our early profiles on this cruise. These can be eliminated by making a shallow lowering to 20 m to dissolve air bubbles adhering to the manifold tubing and the reagent containers, and then returning the instrument to the surface to begin the cast. They are rarely seen on up-casts.

The nitrate data must be corrected for the relatively long lag time that occurs as the sample flows from the inlet to the detector. If the lag time is not adjusted for properly, then large offsets result between up- and down-cast data when the nitrate data is plotted vs temperature, especially in areas with large gradients. The lag time for the nitrate channel was determined in two ways. The simplest approach was to measure the time required for a bubble to flow from the inlet to the detector. The lag time was also determined empirically by adjusting the offset between nitrate and temperature until the up- and down-casts agreed as closely as possible when nitrate was plotted vs temperature. The same estimate of the lag time (65 s) was obtained by both methods. Plots of nitrate vs temperature for both the down- and up-casts do not overlap exactly, even when the lag time is adjusted to minimize the differences (Fig. 5). Similar differences in the salinity vs temperature plots (Fig. 5) suggest that the offsets are real.

Mixing of the sample within the reaction manifold will occur to some extent during the 65 s required for the sample to flow from the inlet to the detector. This mixing limits the vertical resolution of chemical structure that can be achieved. The effects of this mixing on the response rate of the instrument can be assessed from the signal change that was observed during the analysis of standards. The valves that were used to switch between samples and standards were placed in the manifold as close to the sample inlet as possible. The standards were exposed to essentially the same flow regime as were the samples. Switching the valves therefore had an effect that was equivalent to a step increase or decrease in concentration at the sample inlet. A standard curve that was

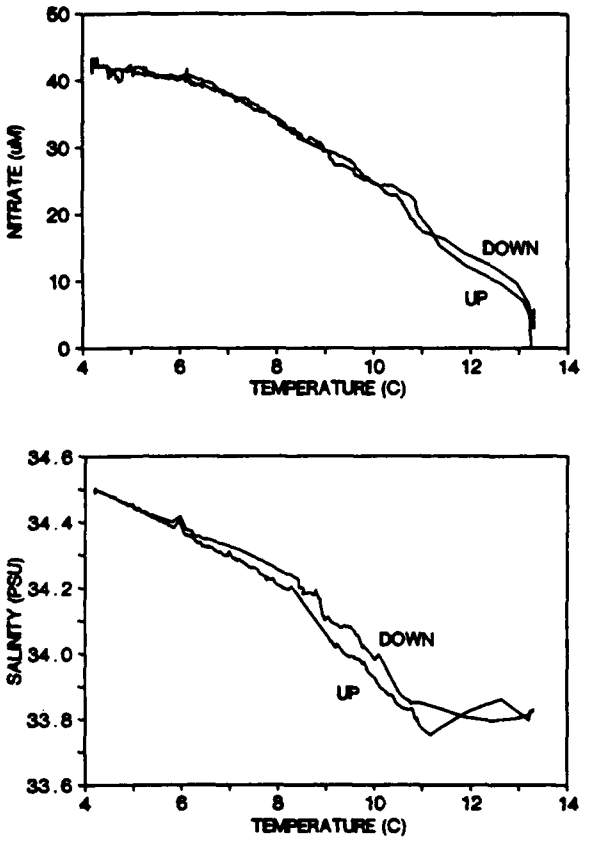

Fig. 5. Nitrate and salinity plotted vs temperature for the down- and up-casts.

obtained *in situ* is shown in detail in Fig. 2. Plots of the logarithm of nitrate vs time are nearly linear during the period when the concentration is changing, with the exception of the first 1 or 2 data points. Linear regressions of the logarithm of the nitrate concentration vs time for each of the three step changes in concentration shown in Fig. 2 gave slopes from 0.1 to 0.12 s^{-1}. Eight to 10 s (1/slope) are required for the detector to sense a concentration change corresponding to 63% (1–1/e) of the step change and 34–40 s are required for the detector response to reach 98% of the steady-state value. Eight seconds correspond to 5 m at a lowering rate of 40 m min^{-1} and features on this scale should be detectable, but not fully resolved.

The data obtained as the Scanner passed through the thermocline confirm the response rate of the nitrate analyses. The temperature drop in the thermocline was 2°C from 18 to 28 m and 30 s were required to lower the instrument through this depth range at 20 m min^{-1}. The nitrate profile through the thermocline was very similar to that observed for temperature. However, the increase in nitrate concentrations from 2 μM in the surface layer on the up-cast to 22 μM below the thermocline was spread over a distance of 16 m or a time of 48 s. This is larger than the minimum time of 34–40 s that would be required to fully resolve the nitracline if it were a vertical step. The extra few seconds required to

resolve the nitrate increase were probably due to the fact that the concentration change was not a step function.

Close inspection of the nitrate data on the down-cast shows that the concentration began to increase before the temperature as the instrument entered the thermocline (Fig. 4). Again, this is probably an artifact due to mixing in the reaction manifold. Flow velocities in the center of the capillary tubing are approximately two times the mean velocity (RUZICKA and HANSEN, 1988). There is a potential for high nitrate water that is sampled as the system moves down into the thermocline to be mixed with low nitrate water further ahead in an analytical system. Thus the system can have both a memory effect due to samples lagging behind in the reaction manifold and also an "anticipation" of the concentrations to come over the next 65 s if some of the sample entering the inlet is rapidly mixed forward to combine with the bulk of the sample nearing the detector. These effects tend to be minimized by the small diameter of the manifold tubing (RUZICKA and HANSEN, 1988), but they are not eliminated.

CONCLUSION

Nitrate concentrations can be measured *in situ* through steep temperature and chemical gradients with a relatively simple continuous flow analyser. Although the system cannot provide as great a resolution of vertical nitrate structure as can temperature or conductivity sensors, the vertical extent of the nitracline was probably resolved to within about 5 or 6 m. Improved vertical resolution can be obtained at slower lowering rates. As our experience with instruments of this type grows, we can expect that the performance will exceed the limits described here. In addition, it will be feasible to analyse an even greater variety of chemical species than are described here (e.g. JOHNSON *et al.*, 1986b).

Acknowledgements—This work was supported by ONR Contracts N00014-82-K-0740 and N00014-86-G-0147. We would like to thank the captain and crew of the R.V. *Pt. Sur* for their generous assistance. We also thank Ginger Elrod and Carol Chin for performing the analyses of the discrete samples and Thomas Chapin, Janey Burger and Nina Greenburg for assistance with sampling and Scanner operations at sea.

REFERENCES

BEN-YAAKOV S. and I. R. KAPLAN (1968) pH–temperature profiles in oceans and lakes using an *in situ* probe. *Limnology and Oceanography*, **13**, 688–693.

BERELSON W. M. (1985) Studies of water column mixing and benthic exchange of nutrients, carbon and radon in the Southern California Borderland. Ph.D. thesis, University of Southern California, Los Angeles, 219 pp.

FOYN E. (1965) The oxymeter. In: *Progress in oceanography*, Vol. 3, M. SEARS, editor, Pergamon Press, Oxford, pp. 137–144.

JOHNSON K. S. and R. L. PETTY (1983) Determination of nitrate and nitrite in seawater by flow injection analysis. *Limnology and Oceanography*, **28**, 1260–1266.

JOHNSON K. S., C. L. BEEHLER, C. M. SAKAMOTO-ARNOLD and J. J. CHILDRESS (1986a) *In situ* measurements of chemical distributions in a deep-sea hydrothermal vent field. *Science*, **231**, 1139–1141.

JOHNSON K. S., C. M. SAKAMOTO-ARNOLD and C. L. BEEHLER (1986b) A submersible flow analysis system. *Analytica Chimica Acta*, **179**, 245–257.

JOHNSON K. S., J. J. CHILDRESS, R. R. HESSLER, C. M. SAKAMOTO-ARNOLD and C. L. BEEHLER (1988) Chemical and biological interactions in the Rose Garden hydrothermal vent field, Galapagos Spreading Center. *Deep-Sea Research*, **35**, 1723–1744.

KESTER D., K. T. CROCKER and G. R. MILLER, Jr (1973) Small-scale oxygen variations in the thermocline. *Deep-Sea Research*, **20**, 409–412.

RUZICKA J. and E. H. HANSEN (1988) *Flow injection analysis*, 2nd edn, Wiley, New York, 498 pp.

Deep-Sea Research, Vol. 36, No. 2, pp. 241–254, 1989.
Printed in Great Britain.

0198-0149/89 $3.00 + 0.00

Hydrogen peroxide in the western Mediterranean Sea: a tracer for vertical advection

KENNETH S. JOHNSON,* STEWART W. WILLASON,† DENIS A. WIESENBURG,‡§
STEVEN E. LOHRENZ‡‖ and ROBERT A. ARNONE‡

(*Received* 27 *November* 1987; *in revised form* 8 *September* 1988; *accepted* 14 *September* 1988)

Abstract—Hydrogen peroxide, micronutrients, chlorophyll, primary production and light were measured at a series of stations in the western Mediterranean Sea. Hydrogen peroxide concentrations greater than 100 nmol l^{-1} were found in this region. There was a significant relationship between hydrogen peroxide and primary production rates near the surface where the light intensity was high. This link between hydrogen peroxide and biological activity may have resulted from photochemically reactive organic compounds that were excreted during photosynthesis or from the direct biological production of hydrogen peroxide. Elevated concentrations were not found in the deep chlorophyll maximum however, which indicates that high light intensities are necessary for biogenic hydrogen peroxide production in this area. Hydrogen peroxide concentrations decreased much more slowly with depth than did light. The decoupling of light and hydrogen peroxide must have been due to a combination of a slow decay rate and rapid vertical transport. However, simple calculations indicate that eddy diffusion alone could not have transported enough hydrogen peroxide to produce the effects that were seen. Large anomalies in the concentration profiles that were detected in frontal regions indicate that hydrogen peroxide can be a useful tracer of vertical transport in the upper ocean. The size of the anomalies appears to be coupled to the salinity gradient across the front, which drives the frontal circulation.

INTRODUCTION

HYDROGEN peroxide is an ubiquitous component of the surface waters in temperate and tropical oceans. It has been found in the Gulf of Mexico (VAN BAALEN and MARLER, 1966; ZIKA *et al.*, 1985a), Atlantic (COOPER *et al.*, 1987) and Pacific (ZIKA *et al.*, 1985b; JOHNSON *et al.*, 1988) Oceans and in the Mediterranean Sea (JOHNSON *et al.*, 1988). Concentrations measured at the surface range from 10 to 300 nmol l^{-1}. Its concentration decreases at a near exponential rate with depth and is usually undetectable below 150 m. Oceanographic distributions of hydrogen peroxide and laboratory experiments indicate that it is produced by photochemical reactions involving dissolved organic compounds. The concentration increases linearly with the solar flux and the rate of increase is greatest in water with a high dissolved organic matter (DOM) concentration (MOPPER and ZIKA, 1987; PETASNE and ZIKA, 1987). Its presence in the water column also may be coupled directly to the biological cycle (PALENIK *et al.*, 1987; ZEPP *et al.*, 1987). Photorespiration by algae at high light intensities results in intracellu-

* Moss Landing Marine Laboratories, P.O. Box 450, Moss Landing, CA 95039, U.S.A.
† Marine Science Institute, University of California, Santa Barbara, CA 93106, U.S.A.
‡ Ocean Sciences Directorate, Naval Ocean Research and Development Activity, SSC, MS 39529, U.S.A.
§ Department of Oceanography, Texas A&M University, College Station, TX 77843, U.S.A.
‖ Center for Marine Studies, University of Southern Mississippi, SSC, MS 39529, U.S.A.

lar hydrogen peroxide production (HARRIS, 1979; OGREN, 1984) that may "leak" into the water column. In addition, biogenic compounds present in seawater can act as photosensitizers that lead to its production (MOPPER and ZIKA, 1987).

The continuous decrease in hydrogen peroxide concentrations with depth led us to investigate whether it can be used as a tracer for vertical advection near the surface. The hydrogen peroxide concentration in vertically displaced bodies of water should differ from that of the surrounding water. These anomalies could be used to identify episodic processes that transport nutrients into the euphotic zone (KLEIN and COSTE, 1985). The utility of this chemical as a tracer of vertical transport depends on its rate of *in situ* formation and decomposition.

We measured the vertical distribution of hydrogen peroxide at a series of stations in the western Mediterranean Sea. A strong salinity and density front exists in this region between Mediterranean Surface Water (MSW) and the Modified Atlantic Water (MAW) that flows into the western Mediterranean Sea through the Straits of Gibraltar (CHENEY and DOBLAR, 1982; LAVIOLETTE, 1987). A sharp frontal boundary was maintained from 2°W to 3°E during our study (LOHRENZ *et al.*, 1988; ARNONE *et al.*, 1988; Fig. 1). The density structure of this frontal system is somewhat similar to that formed by western boundary currents such as the Gulf Stream. However, in contrast to western boundary current systems, the density difference across the Mediterranean front is the result of a strong salinity gradient. The MSW is characterized by salinities >37.5, while the MAW has a salinity of 36.5. The temperature contrast across the front was small (<0.5°C) at the time of our study.

Our measurements have been used to examine the processes that produce hydrogen peroxide in the ocean and to determine the feasibility of using it as a tracer of vertical motions in the upper ocean. We selected a frontal system for this study because they are

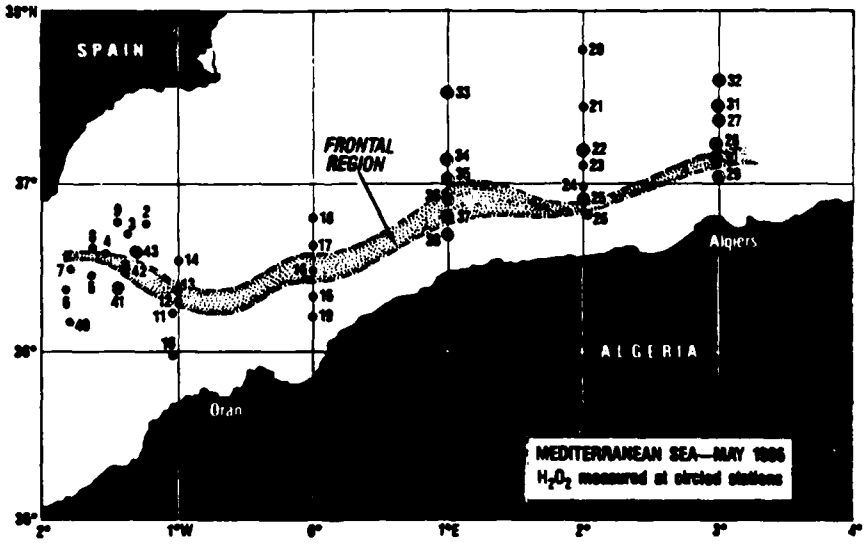

Fig. 1. Station locations in the western Mediterranean Sea during May 1986. Stations where complete hydrogen peroxide profiles were measured are circled. Stippled area shows the location of the front in this region, which was defined by large horizontal salinity gradients.

characterized by relatively high vertical velocities (PINGREE *et al.*, 1974; BOWMAN and ESAIAS, 1978).

METHODS

Measurements of hydrogen peroxide were carried out from 2 May to 21 May 1986 at 17 stations (Fig. 1). Stations were arranged in a series of lines across the frontal system in the study area. Water samples were collected at depths from 1 to 100 m with a submersible pumping system (LOHRENZ *et al.*, 1988). A Neil Brown Mark III CTD was used to determine conductivity, temperature and depth at the pump inlet. *In vivo* chlorophyll fluorescence was determined simultaneously with a SeaMarTech Model 6000 fluorometer on the CTD package. The temperature, salinity (practical salinity units, PSU) and fluorescence structure were determined on each down cast. The pump and CTD were then raised in 5–10 m depth increments and held at each depth for a period of time sufficient to flush the pumping system and obtain one or more samples. The sampling depths (15–17 per cast) were selected to maximize our vertical resolution in the vicinity of the subsurface chlorophyll fluorescence maximum.

Hydrogen peroxide concentrations were measured automatically in the pump effluent every 4 min by flow injection analysis with photometric detection (JOHNSON *et al.*, 1988). The colored condensation product of *N*-ethyl-*N*-(sulfopropyl)aniline and 4-aminoantipyrene formed in the presence of hydrogen peroxide and peroxidase was used to determine the hydrogen peroxide concentration. The detection limit was 12 nmol l^{-1}, which corresponded to three standard deviations of the blank. By comparing the concentrations determined in the pump effluent with the concentration in bucket samples collected next to the pump intake at the surface, the pumping system was demonstrated not to contaminate the hydrogen peroxide samples (JOHNSON *et al.*, 1988).

In addition, nitrate and silicate were determined in the pump effluent by flow injection analysis at 1 min time intervals (JOHNSON *et al.*, 1985). One liter samples were collected for chlorophyll determinations, filtered on Whatman GF/F filters, extracted with acetone for 24 h at –15°C, and analysed at sea (LOHRENZ *et al.*, 1988). ^{14}C-derived primary production was determined near the surface, at the fluorescence maximum and at an intermediate depth at each daylight station (LOHRENZ *et al.*, 1988). Light profiles were measured at each daylight station on a separate cast using a spectral radiometer (ARNONE *et al.*, 1986). Incident solar radiation was measured continuously throughout the cruise with an Eppley pyroheliometer.

Hydrogen peroxide production and decay rates were determined by incubating seawater samples from the surface and from 250 m. Surface samples were collected immediately before the experiment began. The deep seawater was stored in the dark at room temperature for 9 days before the experiment began. Samples were placed in clear, 500 ml polycarbonate bottles and incubated under natural sunlight at 15°C in the same apparatus used for primary production measurements (LOHRENZ *et al.*, 1988). Blue polycarbonate sheets (Acrylite 625-5) were used to attenuate the light levels in one incubator to near those observed at 30 m. Light attenuation in this incubator was determined with a cosine corrected PAR light meter (Biospherical, QCP 200L). In addition, a surface sample was placed in the incubator in a polycarbonate bottle covered with black tape as a dark control. The contents of the bottles were analysed periodically for hydrogen peroxide as described above.

RESULTS AND DISCUSSION

We shall consider first the processes that control the hydrogen peroxide distributions at stations near the ends of the station lines where the front is weak or absent. We will then examine the hydrogen peroxide distributions within the frontal zone itself.

Hydrogen peroxide away from the frontal zone

The concentrations of hydrogen peroxide measured in the western Mediterranean Sea at a series of stations away from the frontal boundary agreed reasonably well with the values measured by ZIKA *et al.* (1985a) in oligotrophic waters of the Gulf of Mexico (Fig. 2). Although our knowledge of the oceanic chemistry of hydrogen peroxide is limited, we would expect a rough correspondence in waters with similar optical properties. As expected, the concentrations decay with depth. An exponential function

$$\ln H_2O_2 \text{ (nmol } l^{-1}) = 4.707 - 0.015 \times Z \text{ (m)}, R^2 = 0.96 \quad (1)$$

was fitted to the profiles in Fig. 2 by least-squares.

The diffuse attenuation coefficient of light at 480 nm, determined from exponential fits to the light profiles measured at the stations occupied during daylight, ranged from –0.04 in the MSW to –0.10 m^{-1} in the MAW. The light intensity at these stations decreased much more rapidly than did the hydrogen peroxide concentration (Fig. 2). The slower

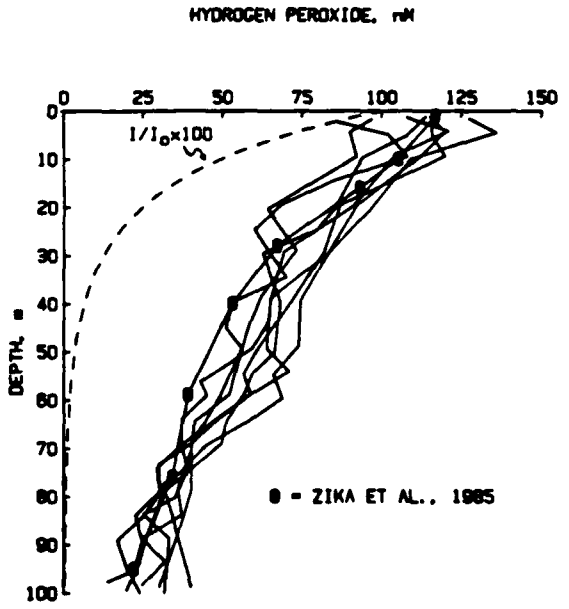

Fig. 2. Hydrogen peroxide concentration profiles vs depth measured at Stas 27, 28, and 31–35. These stations are located away from the influence of the frontal region. Each profile consists of 17 data points, each of which is usually the average of two or more measurements. Individual points are not shown for clarity. The profile measured by ZIKA *et al.* (1985a) at Sta. 1′ in oligotrophic waters of the Gulf of Mexico is shown for comparison. The dashed line is the ratio of the light intensity at depth to the surface intensity, expressed as a percentage, for a diffuse attenuation coefficient of –0.07 m^{-1}. This was a typical value for the area.

decline of the concentration with depth, as compared to light, could have been the result of three factors: (1) Biological production of hydrogen peroxide in the subsurface chlorophyll maximum may have contributed to the relatively slow decay of the concentrations with depth (PALENIK *et al.*, 1987; ZEPP *et al.*, 1987). (2) Vertical mixing could have transported hydrogen peroxide down below the depth at which it was produced, resulting in a slower decrease with depth than that of light (PLANE *et al.*, 1987). (3) Production may not have been a linear function of light intensity. For example, the concentration of dissolved organic compounds, which are required for hydrogen peroxide production (PETASNE and ZIKA, 1987; MOPPER and ZIKA, 1987), may have increased with depth. We will consider the importance of these factors in the ensuing discussion.

A direct link between biological activity and hydrogen peroxide in the ocean has not been demonstrated (ZIKA *et al.*, 1985a, b; COOPER *et al.*, 1987), although hydrogen peroxide production occurs in laboratory cultures of some phytoplankton (PALENIK *et al.*, 1987; ZEPP *et al.*, 1987). We examined our data for a relationship between various indices of biological activity and hydrogen peroxide. A subsurface chlorophyll maximum was present between 25 and 80 m at all the stations (e.g. Fig. 3). Carbon fixation rates (mg C m^{-3} d^{-1}) were 2–10 times higher in samples from this subsurface maximum layer than at the surface (LOHRENZ *et al.*, 1988). There appeared to be no consistent evidence for elevated levels of hydrogen peroxide in the subsurface chlorophyll maximum. To quantify the data, we pooled the hydrogen peroxide concentrations measured in each 10 m depth increment at all stations into two groups: those from a chlorophyll maximum and those from outside the maximum. There were no statistical differences (*t*-test) between the mean hydrogen peroxide concentrations measured in the chlorophyll maximum and those measured outside of it (Table 1). Detectable hydrogen peroxide anomalies were not present in the subsurface chlorophyll maximum layer.

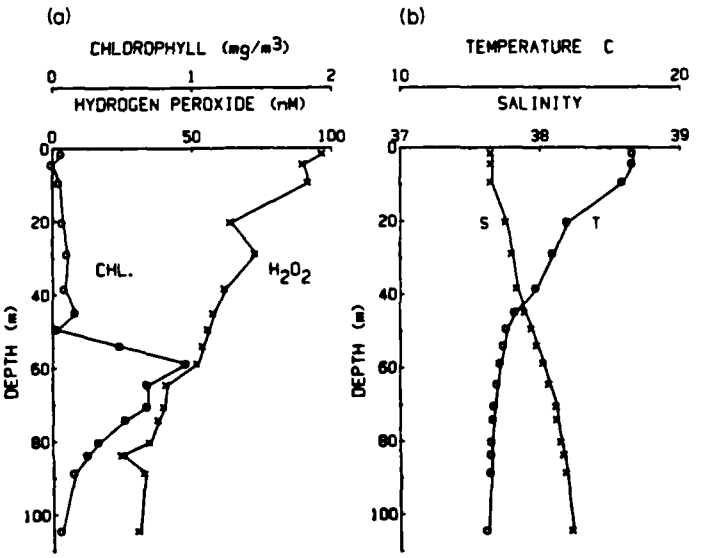

Fig. 3. Profiles of temperature and salinity (a) and hydrogen peroxide and chlorophyll (b) measured at Sta. 34 (37°08.31N, 000°59.94E, 19 May 1986).

Table 1. Comparison of hydrogen peroxide concentrations measured in seawater from the deep chlorophyll maximum and in seawater without elevated chlorophyll concentrations. Samples were defined as coming from the chlorophyll maximum layer if the chlorophyll concentration was greater than 25% of the maximum concentration on that profile

Depth range (m)	Hydrogen peroxide (nmol l^{-1}) Chl. Max.			Background		
	Mean	S.D.	*N*	Mean	S.D.	*N*
20–29	75	12	8	77	10	15
30–39	69	14	15	69	6	10
40–49	53	13	15	62	10	13
50–59	46	18	15	55	14	12
60–69	44	9	18	36	12	9
70–79	37	9	13	38	7	11
80–89	28	5	4	32	12	11

There was a link between rates of primary production and the concentration of hydrogen peroxide near the surface (Fig. 4). The correlation between the hydrogen peroxide concentration and the carbon fixation rate for the samples from the upper 10 m is significant ($P < 0.01$) when Sta. 41 is excluded. In contrast to the situation at the surface, the correlation between the hydrogen peroxide and carbon fixation is not significant for samples from 45 to 55 m (Fig. 4). We believe that there is sufficient reason for excluding the Sta. 41 data from the regression of the near-surface data. There can be a significant correlation between the *concentration* of hydrogen peroxide and the *rate* of carbon fixation only if the effects of primary production on chemical distributions are integrated over a sufficiently long time. There is evidence, discussed below, that the relatively high carbon fixation rate at Sta. 41 was a transient response to a pulse of high nutrient water into the euphotic zone that had occurred recently. There may not have been enough time to affect the hydrogen peroxide distribution. The hydrographic data from Sta. 41 were also anomalous compared to the other stations shown in Fig. 4. For example, Sta. 41 had the lowest surface salinity (36.47) encountered on the cruise. The

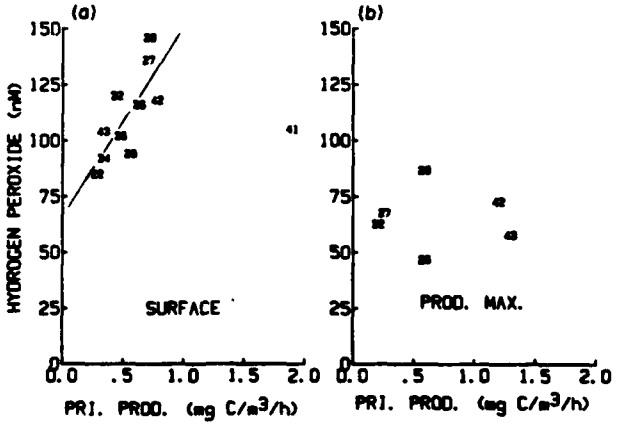

Fig. 4. Hydrogen peroxide concentrations measured at depths between 5 and 10 m (a) and between 45 and 55 m (b) vs the primary production rate measured in the same samples. The number indicates the station where the measurements were obtained. The line through the surface data $H_2O_2 = 66 + 85 \times PP$, $R = 0.76$ was fitted by least-squares after excluding the point at Sta. 41.

surface salinities at the other stations used in Fig. 4 were greater than 37.0, with one exception (36.77 at Sta. 29). The water at Sta. 41 had a much higher percentage of MAW than at any of the other stations.

The strong correlation between hydrogen peroxide and primary productivity that existed only near the surface implies that both high light and high carbon fixation rates are required to increase hydrogen peroxide concentrations. Apparently, either phytoplankton release organic carbon compounds that are photochemically reactive or metabolism at high light levels leads to biological hydrogen peroxide production. Riboflavin is one possible precursor compound that might be responsible for elevated hydrogen peroxide concentrations. It is photochemically reactive, producing approximately 10 nmol l^{-1} H_2O_2 for every 1 nmol l^{-1} added to seawater (MOPPER and ZIKA, 1987). A number of marine organisms produce and excrete riboflavin, and it has been found in seawater (DUNLAP and SUSIC, 1985; MOPPER and ZIKA, 1987). Alternatively, hydrogen peroxide may be produced directly by organisms. Extracellular production of hydrogen peroxide by the marine phytoplankter *Hymenomonas carterae* has been demonstrated in the absence of light (PALENIK *et al.*, 1987). Rates of production extrapolated from the laboratory to the field could be as high as 1–2 nmol l^{-1} h^{-1}.

However, mechanisms involving production in the dark do not explain fully the linkage between hydrogen peroxide concentrations and carbon fixation rates that occur only at the surface. The photorespiration cycle of phytoplankton involves hydrogen peroxide production during glycolate oxidation (LEHNINGER, 1970)

$$CH_2OHCOOH + O_2 \xrightarrow{\text{glycolate oxidase}} CHOCOOH + H_2O_2.$$

The rate of photorespiration increases at high light intensities, where it may function to dissipate excess light energy (HARRIS, 1979), although the exact role is not clear (OGREN, 1984). This cycle could explain the linkage between primary production, light and hydrogen peroxide. However, there is no proof of a direct linkage between photorespiration and extracellular hydrogen peroxide.

Vertical transport may be an important factor in controlling the shape of the hydrogen peroxide concentration profiles (PLANE *et al.*, 1987). We estimated vertical hydrogen peroxide transport with a simple diffusion-reaction model. At steady state, there is a balance between the rate of removal due to diffusive transport and the *in situ* reaction rate

$$dH_2O_2/dt = 0 = K_z\, d^2H_2O_2/dZ^2 - R. \quad (2)$$

K_z is the eddy diffusion coefficient and R is the net *in situ* reaction term for both production and decay reactions. We calculated $d^2H_2O_2/dZ^2$ to be 0.023 nmol l^{-1} m^{-2} at 5 m using equation (1). There is considerable uncertainty regarding the magnitude of the eddy diffusion coefficient in the surface ocean. Using measurements of turbulent energy dissipation and stratification for a variety of surface ocean environments, DENMAN and GARGETT (1983) estimated K_z from 0.3 to 700 m^2 d^{-1} with the larger values acquired during high winds. If a relatively large eddy diffusion coefficient of 90 m^2 d^{-1} is assumed for Mediterranean surface waters, then the rate of change in hydrogen peroxide concentration due to eddy diffusion was 1.9 nmol l^{-1} d^{-1} at 5 m. The effects of diffusion would have to be integrated over several weeks to affect the hydrogen peroxide profile. However, eddy diffusion models may not accurately characterize turbulent mixing and

transport in the upper ocean. PLANE *et al.* (1987) have shown that convective overturn, caused by nocturnal cooling, can transport significant amounts of hydrogen peroxide to depth. KLEIN and COSTE (1985) suggest that unsteady forcing by winds also may result in significant vertical advective transport of chemicals. Clearly, further work needs to be done to characterize chemical transport in the upper ocean.

The photochemical production of hydrogen peroxide in Mediterranean Sea water was observed (Fig. 5) by performing an incubation experiment with seawater collected at the surface (Sta. 19) and at a depth of 250 m (Sta. 1). Hydrogen peroxide concentrations in the incubated samples were linearly related to the solar flux measured with the pyroheliometer, within the precision of our data, and there was no difference between production rates in surface and deep samples (Fig. 6). The mean rate of increase was 9 nmol l^{-1} h^{-1}, averaged over the daylight period. These results should be considered preliminary for several reasons. The incubator blocked a significant amount of ultra violet light, which may have resulted in low production rates. There also may have been container effects, such as trace metal or organic contamination, which would bias the results.

Hydrogen peroxide began to decay at an average rate of 7.2 ± 0.6 nmol l^{-1} h^{-1} (1 S.D.) shortly after sunset in the three samples that reached concentrations greater than 100 nmol l^{-1}. The concentrations in the fourth sample fluctuated near the detection

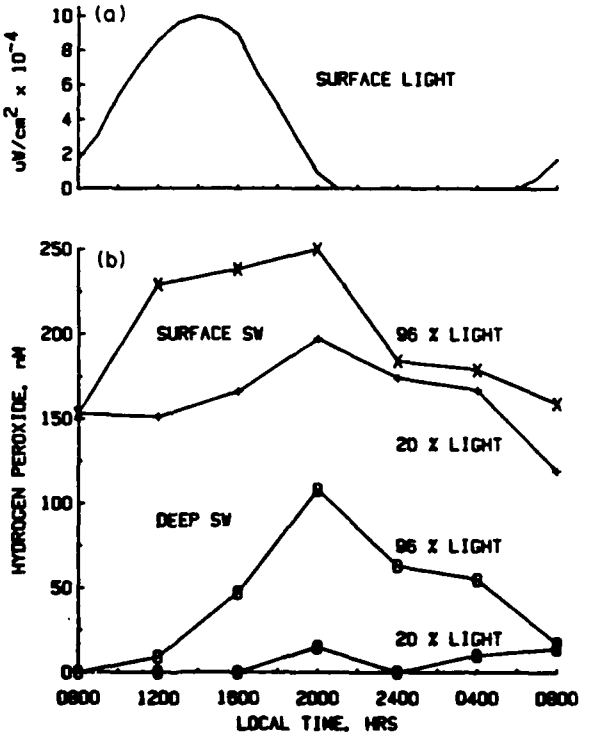

Fig. 5. Results of the seawater incubation experiment. (a) The incident solar radiation throughout the day. (b) The hydrogen peroxide concentrations measured over the course of the day in samples of surface and deep seawater incubated at 96 and 20% of the surface light intensity.

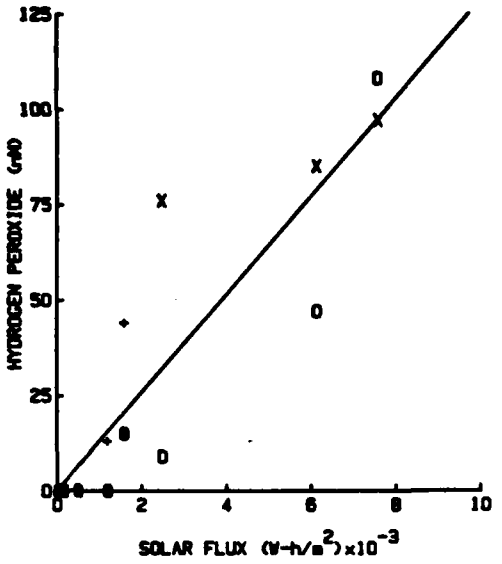

Fig. 6. Hydrogen peroxide concentrations measured during daylight hours in incubated samples vs solar flux estimated in each incubator. Symbols are the same as in Fig. 5. The concentrations in the surface samples were reduced by 153 nmol l^{-1} to correct for the initial concentration of hydrogen peroxide. The solid line through the data $H_2O_2 = -1 + 1.29 \times$ solar flux, $R = 0.88$ was fitted by least-squares to the data in the figure.

limit. The concentration in the dark control bottle decreased continuously at a rate of 3.8 nmol l^{-1} h^{-1} over the 24 h experiment. PLANE *et al.* (1987) refer to a hydrogen peroxide "dark decay life-time" of hours to weeks in the ocean, and use a value of 4 days as average. The initial concentrations in surface water samples (90–150 nmol l^{-1}) would have reached zero after 23–39 h if they decayed linearly at the same rate (3.8 nmol l^{-1} h^{-1}) observed in the dark control. If the concentration decay were exponential, then even longer times would have been required to reach zero concentration. The dark decay rate in the surface samples was greater than the production rate during the late afternoon and evening. However, the concentration did not begin to decrease in any of the samples until sunset. Similar results were obtained in the model simulations by PLANE *et al.* (1987). It is interesting to note that the concentrations returned to near their starting values over a 24 h light cycle. Apparently, the hydrogen peroxide concentration was in a steady state.

These limited results support the view that hydrogen peroxide production is linearly related to light intensity and that it is produced at the same rate in surface and deep water samples. A dramatic increase in the rate of hydrogen peroxide production in deep water, therefore, probably does not explain the differences in the vertical distributions of light and hydrogen peroxide concentrations (e.g. Fig. 2).

Hydrogen peroxide in frontal systems

Hydrogen peroxide appears to be a useful tracer of vertical advective mixing in the Mediterranean. We have not identified any production mechanism that could create concentration maxima in the profiles at depths below 20 or 30 m. The rates of production

and decay are slow enough that time periods of several hours to a few days are necessary for the concentration to come to a steady-state balance between reaction and vertical transport. As a result, the hydrogen peroxide concentration acts as a recorder of a samples recent depth history in the photic zone. If a body of water is rapidly displaced vertically, then its hydrogen peroxide concentration should be different than that of the surrounding water. The magnitude of the concentration difference will depend on the vertical distance traveled by the water body, and on the amount of time elapsed since the displacement.

Large subsurface maxima and minima were present in many of the hydrogen peroxide profiles measured within the frontal system, in contrast to profiles at stations away from the front. For example, a maximum was present below 85 m at Sta. 41 and a minimum occurred between 50 and 70 m at Sta. 43 (Fig. 7). The concentrations in these depth ranges were significantly different ($P < 0.005$, t-test) from the mean of the values measured at the same depths in the set of stations away from the front. The concentrations measured at other depths at Stas 41 and 43 were similar to the concentrations measured away from the front.

The large concentration anomalies in the bands (labeled B at Sta. 41 and band A at Sta. 43; Fig. 7) suggest that these bands of water had undergone recent, rapid vertical displacements. To study this question further, we prepared contoured sections of hydrogen peroxide, nitrate, chlorophyll and density for the line through Stas 41–43 (Fig. 8). This line of stations crossed the front in a region where the greatest horizontal gradients of salinity were found. The contours of the chemical properties clearly show two interleaving bands of water in the front that were centered on the anomalies in the

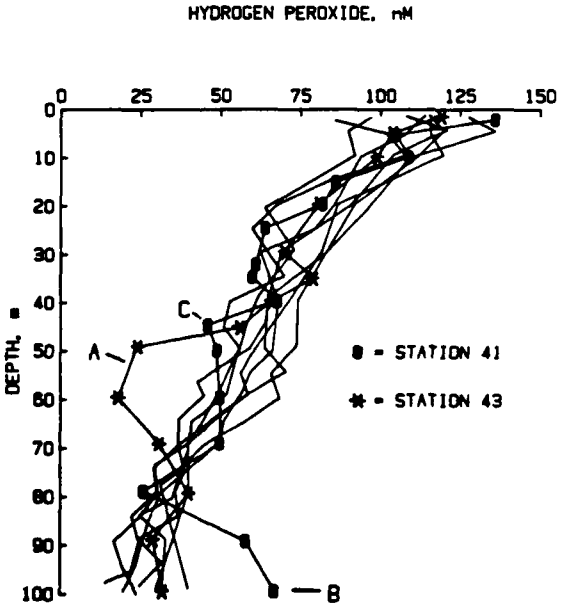

Fig. 7. Hydrogen peroxide concentration profiles measured at Stas 41 (36°22.32N, 001°25.36W, 21 May 1986, 0709 GMT) and 43 (36°36.30N, 001°17.67W, 21 May 1986, 1305 GMT) are shown superimposed on the set of profiles measured away from the influence of the front.

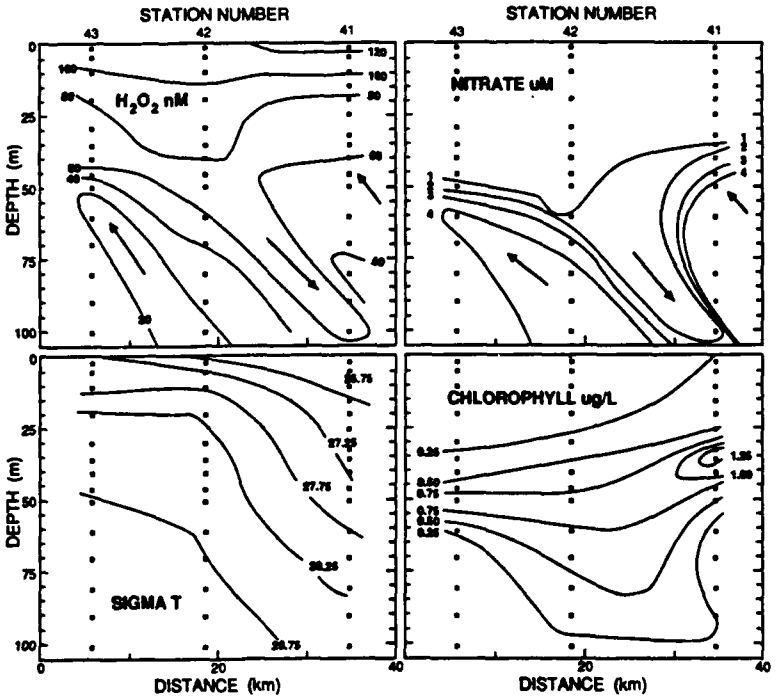

Fig. 8. Contoured sections of properties along the line through Stas 41–43. Units for the contour lines are: H_2O_2, nmol^{-1}; NO_3, μmol l^{-1}; chlorophyll, μg l^{-1}.

hydrogen peroxide profiles. For example, the nitrate concentrations in these bands were substantially different than those in the surrounding water at the same depth (Fig. 8). The anomalies in nitrate concentrations were consistent with the trends expected if these bands had been displaced vertically. The band labeled A in Fig. 7 had low hydrogen peroxide and high nitrate concentrations relative to the surrounding water. These differences indicate this water had been displaced upward shortly before sampling. The water in band B (Fig. 7) must have been displaced downward, as it contained elevated hydrogen peroxide concentrations and low nitrate concentrations. The hydrogen peroxide contours in both bands are parallel to those of density, which suggests that the vertical displacements occurred along isopycnal surfaces.

The size of the chemical anomalies can be used to set limits on the distance of vertical displacement and the time elapsed since the displacement occurred. For example, if the hydrogen peroxide concentration decayed *in situ* at the same rate that we observed in the incubation experiment, then the anomaly in band B would have disappeared in 5–10 hours. The hydrogen peroxide concentration (67 nmol l^{-1}) in band B at 100 m was not significantly different (t-test, $P < 0.05$) from the concentrations measured at depths between 15 and 60 m in the set of stations away from the front. The source of the water in band B therefore must have been at a depth less than 60 m.

The presence of 30% more chlorophyll on the small hydrogen peroxide anomaly ($P < 0.05$, t-test) at Sta. 41 (labeled C in Fig. 7) than that in the surrounding water (Fig. 8) suggests that this upwelled band had been in place long enough for the hydrogen

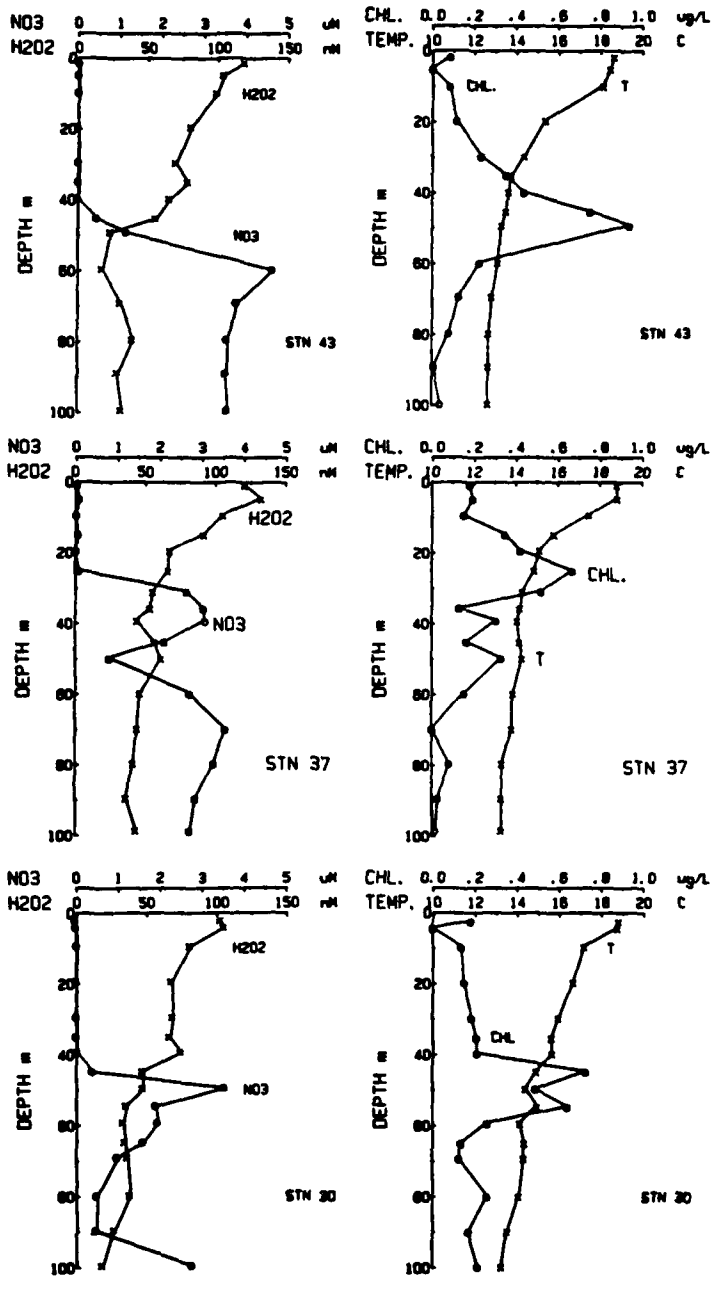

Fig. 9. Concentration profiles of hydrogen peroxide, nitrate, chlorophyll and temperature at Stas 43, 37 and 30, which lie within the frontal zone. Statistically significant anomalies (*t*-test, $P < 0.1$) in hydrogen peroxide occur at Sta. 43 from 50 to 70 m, at Sta. 37 from 30 to 40 m and at Sta. 30 from 50 to 60 m.

peroxide concentration to increase (by photoproduction or vertical transport) and the phytoplankton to respond to the presence of high nutrients at a relatively shallow depth. Given typical plankton doubling times of one per day, only 8 h of daylight would be required for the observed increase in chlorophyll concentration. In fact, the upward pulse of nutrients in this band may have been partially responsible for the high productivity value that caused this station to deviate from the primary production–hydrogen peroxide relationship found at other stations (Fig. 4).

Maxima and minima were present in temperature, salinity and nutrient profiles at all of the frontal stations. However, the size of the anomalies in the hydrogen peroxide profiles diminished and finally disappeared from west to east in the frontal stations (Fig. 9). The residence time of water in the up- and down-welled masses must have increased to the east along the front, which allowed the hydrogen peroxide to approach equilibrium with the surrounding water. The surface salinity gradient across the front also weakened from west to east (0.047 km^{-1} at Stas 41–43, 0.016 km^{-1} at Stas 36–38 and 0.013 km^{-1} at Stas 28–29). The decreasing salinity gradient to the east probably resulted in slower vertical velocities and small hydrogen peroxide anomalies as it is the salinity gradient that drives the frontal circulation.

CONCLUSIONS

Our measurements have shown hydrogen peroxide concentrations in the western Mediterranean Sea greater than 100 nmol l^{-1}. The decoupling of light and hydrogen peroxide must be due to the combination of vertical transport and the relatively slow consumption rate (3–7 nmol l^{-1} h^{-1}). However, the changes in hydrogen peroxide concentration calculated from eddy diffusion models were not large enough to transport significant amounts of H_2O_2 to depth. Additional mechanisms of transport, perhaps based on advective processes, must transport hydrogen peroxide vertically in this region.

There appeared to be a link between primary production and the hydrogen peroxide concentration at the surface. This link may have been due to the presence of organic compounds produced during photosynthesis that acted as photosensitizers or due to the direct biological production of hydrogen peroxide. Because the linkage is found only at the surface, it cannot explain the slower decrease in concentration with depth, as compared to light.

Finally, hydrogen peroxide appears to have considerable potential as a tracer for vertical motions near the sea surface. The anomalies in hydrogen peroxide concentrations that result when water is advected vertically can be used to determine the time elapsed since the displacement when the *in situ* reaction rates are known. The size of the anomalies appears to be directly coupled to the strength of the frontal circulation.

Acknowledgements—This work was supported by ONR Contract N00014-82-K-0740 to KSJ and by ONR Program Element 61153N, through the NORDA Defense Research Sciences Program.

REFERENCES

ARNONE R. A., R. R. BIDIGARE, C. C. TREES and J. M. BROOKS (1986) Comparison of the attenuation of spectral irradiance and phytoplankton pigments within frontal zones. *Society of Photo-Optical Instrumentation Engineers*, 637, 126–130.

ARNONE R. A., D. A. WIESENBURG and K. D. SAUNDERS (1988) Origins of the Algerian Current. *Journal of Geophysical Research*, submitted.

BOWMAN M. J. and W. E. ESAIAS (1978) *Oceanic fronts in coastal processes*, Springer-Verlag, New York, 114 pp.

CHENEY R. E. and R. A. DOBLAR (1982) Structure and variability of the Alboran Sea frontal system. *Journal of Geophysical Research*, **87**, 585–594.

COOPER W. J., E. S. SALTZMAN and R. G. ZIKA (1987) The contribution of rainwater to variability in surface ocean hydrogen peroxide. *Journal of Geophysical Research*, **92**, 2970–2980.

DENMAN K. L. and A. E. GARGETT (1983) Time and space scales of vertical mixing and advection of phytoplankton in the upper ocean. *Limnology and Oceanography*, **28**, 801–815.

DUNLAP W. C. and M. SUSIC (1985) Determination of pteridines and flavins by reverse-phase, high-performance liquid chromatography with fluorimetric detection. *Marine Chemistry*, **17**, 185–198.

HARRIS G. P. (1979) Photosynthesis, productivity and growth: the physiological ecology of phytoplankton. *Archiv fur Hydrobiologie*, **16**, 1–191.

JOHNSON K. S., R. L. PETTY and J. THOMSEN (1985) Flow injection analysis for seawater micronutrients. In: *Mapping strategies in chemical oceanography*, A. ZIRINO, editor, American Chemical Society, Advances in Chemistry Series No. 209, pp. 7–30.

JOHNSON K. S., C. M. SAKAMOTO-ARNOLD, S. W. WILLASON and C. L. BEEHLER (1987) Reversed flow injection: application to the determination of nanomolar levels of hydrogen peroxide in seawater. *Analytica Chimica Acta*, **201**, 83–94.

KLEIN P. and B. COSTE (1984) Effects of wind-stress variability on nutrient transport into the mixed layer. *Deep-Sea Research*, **31**, 21–37.

LAVIOLETTE P. E. (1987) Portion of the western Mediterranean Circulation Experiment completed. *Transactions of the American Geophysical Union*, **68**, 123–124.

LEHNINGER A. L. (1970) *Biochemistry*, Worth, New York, p. 478.

LOHRENZ S. E., D. A. WIESENBURG, I. P. DEPALMA, K. S. JOHNSON and D. E. GUSTAFSON, JR (1988) Interrelationships among primary production, chlorophyll, and environmental conditions in frontal regions of the western Mediterranean Sea. *Deep-Sea Research*, **35**, 793–810.

MOPPER K. and R. G. ZIKA (1987) Natural photosensitizers in sea water: riboflavin and its breakdown products. In: *Photochemistry of environmental aquatic systems*, R. G. ZIKA and W. J. COOPER, editors, American Chemical Society, Washington, D.C., pp. 174–190.

OGREN W. L. (1984) Photorespiration: pathways, regulation and modification. *Annual Reviews of Plant Physiology*, **35**, 415–442.

PALENIK B., O. C. ZAFIRIOU and F. M. M. MOREL (1987) Hydrogen peroxide production by a marine phytoplankter. *Limnology and Oceanography*, **32**, 1365–1369.

PETASNE R. G. and R. G. ZIKA (1987) Fate of superoxide in coastal sea water. *Nature*, **325**, 516–518.

PINGREE R. D., G. R. FORSTER and G. K. MORRISON (1974) Turbulent convergent tidal fronts. *Journal of the Marine Biological Association of the United Kingdom*, **54**, 469–479.

PLANE J. M. C., R. G. ZIKA, R. C. ZEPP and L. A. BURNS (1987) Photochemical modeling applied to natural waters. In: *Photochemistry of environmental aquatic systems*, R. G. ZIKA and W. J. COOPER, editors, American Chemical Society, Washington, D.C., pp. 250–267.

VAN BAALEN C. and J. E. MARLER (1966) Occurrence of hydrogen peroxide in sea water. *Nature*, **211**, 951.

ZEPP R. G., Y. I. SKURLATOV and J. T. PIERCE (1987) Algal-induced decay and formation of hydrogen peroxide in water: its possible role in oxidation of anilines by algae. In: *Photochemistry of environmental aquatic systems*, R. G. ZIKA and W. J. COOPER, editors, American Chemical Society, Washington, D.C., pp. 215–224.

ZIKA R. G., J. W. MOFFETT, R. G. PETASNE, W. J. COOPER and E. S. SALTZMAN (1985a) Spatial and temporal variations of hydrogen peroxide in Gulf of Mexico waters. *Geochimica et Cosmochimica Acta*, **49**, 1173–1184.

ZIKA R. G., E. S. SALTZMAN and W. J. COOPER (1985b) Hydrogen peroxide concentrations in the Peru upwelling area. *Marine Chemistry*, **17**, 265–275.